Hibecovirus (genus *Betacoronavirus*) infection linked to gut microbial dysbiosis in bats

Running title: Coronavirus infection alters bat microbiome

Dominik W. Melville*, Magdalena Meyer*, Alice Risely, Kerstin Wilhelm, Heather J. Baldwin, Ebenezer K. Badu, Evans Ewald Nkrumah, Samuel Kingsley Oppong, Nina Schwensow, Marco Tschapka, Peter Vallo, Victor M. Corman, Christian Drosten, Simone Sommer

* Authors contributed equally

Corresponding Author: Dominik W. Melville, Institute of Evolutionary Ecology and Conservation Genomics, Ulm University, Ulm, BW, 89081, Germany; dominikwerner.schmid@uni-ulm.de

Affiliations: DWM, MM, KW, AR, HJB, NS, MT, PV and SS: Institute of Evolutionary Ecology and Conservation Genomics, Ulm University, Ulm, BW, 89081, Germany.

AR: School of Science, Engineering, and the Environment, Salford University, Salford M5 4NT, UK

HJB: School of Natural Sciences, Macquarie University, Sydney, New South Wales, 2113, Australia

EKB, EEN and SKO: Department of Wildlife and Range Management, Kwame Nkrumah University of Science and Technology, Kumasi, Ghana.

PV: Institute of Vertebrate Biology, Czech Academy of Sciences, Brno, 675 02, Czech Republic.

VMC and CD: Charité – Universitätsmedizin Berlin Institute of Virology, Berlin, Germany and German Centre for Infection Research (DZIF), Berlin, 10117, Germany.

Author Contributions: DWM, MM and SS developed and conceived the idea of the present study. SS, NS and CD acquired funding. HJB, EKB, EEN, SKO, PV, and MT collected field data and archived biological samples. MT and PV organized the field work. KW, DWM and MM completed laboratory work. HJB, VMC and CD generated the infection data. DWM, MM, and AR analyzed the data. DWM, MM and SS wrote the first manuscript draft. All authors contributed to the final version of the manuscript.

Abstract

Little is known about how zoonotic virus infections manifest in wildlife reservoirs. However, a common health consequence of enteric virus infections is gastrointestinal diseases following a shift in gut microbial composition. The sub-Saharan hipposiderid bat complex has recently emerged to host at least three coronaviruses (CoVs), with *Hipposideros caffer D* appearing particularly susceptible to *Hibecovirus* CoV-2B infection. In this study, we complement body condition and infection status data with information about the gut microbial community to understand the health impact of CoV infections in a wild bat population. Of the three CoVs, only infections with the distantly SARS-related *Hibecovirus* CoV-2B were associated with lower body

condition and altered the gut microbial diversity and composition. The gut microbial community of infected bats became progressively less diverse and more dissimilar with infection intensity, arguing for dysbiosis as per the Anna-Karenina principle. Putatively beneficial bacteria, such as from the genera *Alistipes* and *Christensenella*, decreased with infection intensity, while potentially pathogenic bacteria, namely *Mycoplasma* and *Staphylococcus*, increased. Infections with enterically replicating viruses may therefore cause changes in body condition and gut dysbiosis with potential negative health consequences even in virus reservoirs. We argue that high-resolution data on multiple health markers, ideally including microbiome information, will provide a more nuanced picture of bat disease ecology.

Keywords: coronavirus, microbiome, Chiroptera, Anna-Karenina principle, Ghana.

Introduction

A stable and diverse gut microbiome is widely understood to indicate host health [1–3] and determine host fitness [4–6]. Perturbations can lead to idiosyncratic and unstable configurations of the gut microbial community (i.e., dysbiosis following the Anna-Karenina principle: 'all healthy microbiomes are similar; each dysbiotic microbiome is dysbiotic in its own way') [2, 7], and impair metabolic and immunological functions provided by the gut microbiota [8–10]. A possible though not immediately visible health consequence of a virus infection is the reshuffling of the host-associated gut microbiota and gastrointestinal disease [11–13]. However, compared with humans or mice we know very little about how the microbiota of wildlife responds to viral challenges [14–17], and even less is known about how the microbiota of pathogen reservoir hosts copes with virus infections.

Bats count among the best studied virus reservoirs albeit rarely showing signs of disease [18–23]. Compared with the physiological and behavioral responses to infections (e.g., [24, 25]), our knowledge about how the gut microbial community of bats respond to infections is limited [26]. Their short gut transit times [27, 28] and their supposedly low level of phylosymbiosis [29, 30] even brought into question whether bats rely on their gut microbiota [31, 32]. However, the enlarged digestive area by villi in bats offers niches for microbiota in bats [33] and bat gut microbes are enriched in genes supporting nutrient acquisition [34–38] and immunity [39, 40]. Moreover, the study by Liu et al. (2022) attests to a potential role of bat gut microbiota in pathogen tolerance. The researchers transplanted the gut microbiota from wild Great Himalayan roundleaf bats (*Hipposideros armiger*) into antibiotic-treated mice, and found a rapid engagement with cytotoxic innate and adaptive immune pathways, culminating in tolerating a challenge with the influenza virus H1N1 [40]. By contrast, the microbiota shifted towards a

bacterial community dominated by pathogenic taxa in wild Jamaican fruit bats (*Artibeus jamaicensis*) infected with an enteric Astrovirus [41]. To date, the work by Wasimuddin and colleagues (2019) remains the only example to document gut microbial dysbiosis following a virus infection in wild bats, although this shift had no repercussions on host body condition. This paucity of studies investigating bat-microbiome-virus interactions greatly limits our understanding of the role of gut microbiota in resisting, tolerating and clearing virus infections.

Coronaviruses (CoVs) count among the most diverse viral families discovered in bats globally with at least five now known to have crossed species boundaries and spilled over into humans causing mild to severe respiratory tract infections [21, 42, 43]. In humans and non-bat animal hosts, some of these viruses alter the composition of the gut microbial community [44–47], modulating the host's immunological response to the infection [48]. Given that CoVs replicate enterically in bats [49], CoV infections could also feasibly alter their gut microbial community in bats. Cave-dwelling, sub-Saharan roundleaf bats (genus: *Hipposideros*), which form a diverse species complex [50], have recently emerged as ancestral hosts to the *Alphacoronavirus* HCoV-229E, which causes mild cold symptoms in humans [43]. Furthermore, hipposiderids host at least two *Betacoronaviruses*, provisionally termed CoV-2B and CoV-2Bbasal [43, 51, 52]. Interestingly, the viruses show uneven infection patterns among the co-inhabiting *Hipposideros* species: CoV-229E is most prevalent among *Hipposideros (H.) caffer C*, whereas *H. caffer D* is likely the main reservoir host to both *Betacoronaviruses* [51]. Moreover, immune genes involved in adaptive immunity were associated with susceptibility of *H. caffer D* to either SARS-related *Betacoronavirus* [53]. Yet, knowledge about whether the body condition and gut microbiota of such reservoir species changes with CoV infection is lacking.

In this article, we explore the link between two host health markers, i.e., body condition and gut microbial community, and infections with either of three distinct CoVs. First, we assessed whether the body condition of Sundevall's roundleaf bat (*H. caffer D*) infected with either of three distinct CoVs (i.e., the *Hibecoviruses* CoV-2B and CoV-2Bbasal and the *Duvinacovirus* CoV-229E) declined. A change in body condition is an important health indicator in bats [54], although rarely reported so far (but see: [19, 23]). Second, we test whether the diversity and composition of the gut microbiota found in uninfected bats differed from that of bats positive for either of the three CoVs, and whether the change correlates with infection intensity. Because *H. caffer D* was suggested to be the main reservoir to both SARS-related *Betacoronaviruses* [51, 53], we hypothesize that only these infections affect body condition and microbiota. The hypothesis-driven approach and virus screening down to species level sets our work apart from previous research [41]. In addition, linking dysbiosis with infection intensity adds a quantifiable dimension to the Anna-Karenina principle [7]. We leverage virus infection and body condition information from 591 adult bats collected from five cave sites in Ghana between 2010 and 2012 and high quality 16S rRNA microbiome data from a subsample of 218 bats ($n_{uninfected}$=46; n_{CoV2B}=41; $n_{CoV2Bbasal}$=70; $n_{CoV229E}$=61). Our results demonstrate that enterically replicating viruses can alter the body condition and gut microbial community even in virus reservoirs.

Material & Methods

Sampling design

Sampling protocols and methods were described in detail elsewhere [51]. Briefly, bats were captured at five different cave sites in central Ghana, West Africa: Buoyem 1 (N7°72'35.833" W1°98'79.167), Buoyem 2 (N7°72'38.056" W1°99'26.389), Forikrom (N7°58'97.5" W1°87'30.299), Kwamang 1 (N6°58'0.001" W1°16'0.001) and Kwamang 2 (N7°43'24.899" W1°59'16.501) over 12 sampling events spread evenly over the span of two years (September 2010-August 2012). Each sampling event consisted of mist net trapping at the cave entrance one hour after dusk until dawn for two, non-consecutive nights. *H. caffer D* was identified molecularly by sequencing the *cytb* gene from 2mm wing punches collected at sampling [50, 51, 53]. The species nomenclature of the *H. caffer* complex remains unresolved throughout the Afrotropics, but here we use *H. caffer D*, as an interim species name [50, 55]. Additionally, fecal pellets were collected from bats held individually in clean bags until defecation, and stored in RNAlater (Life Technologies, USA) at -80 °C for subsequent virus and microbiome screening [55]. Body mass (g) and forearm length (mm) were taken and used to calculate the body condition index (as body mass/forearm length) for non-pregnant adults. This relationship between body mass and forearm length can be used as proxy to estimate the impact of infections generally [54] and in bats in particular [23]. A higher body condition index implies bats have more fat reserves, possibly indicating superior health [26]. The Wildlife Division of the Forestry Commission of the Ministry of Lands, Forestry and Mines granted Research (A04957) and ethics permit (CHRPE49/09/CITES).

Virus screening

Approximately 20mg of the fecal material was suspended in 500 µl RNAlater stabilizing solution (QIAGEN, Hilden, Germany) and homogenized via vortexing before extracting and purifying viral RNA with the MagNa Pure 96 system (Roche, Penzberg, Germany) [43, 56]. Elation volumes were set at 100 µl. Subsequently, a real-time reverse transcription-PCR assay was designed to detect several *Alphacoronaviruses* and *Betacoronaviruses*, as described previously [43, 52, 55, 57]. In each PCR run, in vitro transcribed and photometrically quantified RNAs (IVTs), generated from TA-cloned periamplicons using the T7-driven MEGAscript (Life Technologies, Heidelberg, Germany), were used as positive controls and calibrators to ensure run-to-run consistency [51, 58]. A total of four CoVs were described: A MERS-related *Betacoronavirus* termed 2C exclusively found in samples originating from *Nycteris macrotis* [55, 57], the *Alphacoronavirus* CoV-229E-like as the closest known ancestral form to the HCoV-229E [43], and two distantly SARS-related *Betacoronaviruses*, named CoV-2B and CoV-2Bbasal [52, 55]. Genome-level analysis according to recent taxonomical amendments assigned both *Betacoronaviruses* to the subgenus *Hibecovirus,* which were previously included in the genus *Sarbecovirus,* and the *Alphacoronavirus* to the subgenus *Duvinacovirus* (author C.D., own unpublished observations). Our focal species *H. caffer D* hosts both *Hibecoviruses* and the *Duvinacovirus* CoV-229E-like [55]. Notably, *H. caffer D* is thought to be particularly susceptible to infections with the *Hibecovirus* 2B [53, 55], which hints at the species' role as main reservoir to this virus. After viral screening, we recorded the infection status (as category, i.e., positive for CoV-229E-like, CoV-2B, or CoV-2Bbasal) and infection intensity estimated based on cycle threshold (CT) value for each sample. Low CT-values imply a more acute infection, and were previously found in *H. caffer D* infected with *Hibecovirus* CoV-2B compared with closely related hipposiderids [55].

16S rRNA sequencing and bioinformatics

A subset of 221 fecal samples representing each infection status with roughly similar sample sizes was chosen for 16S rRNA sequencing. Because of the confounding effect of co-infection [59], samples from bats with more than one virus infection were not included. Bacterial DNA was extracted from the fecal material as per instructions of the NucleoSpin Soil Kit (Macherey-Nagel, Germany). This includes a bead-beating step to mechanically lyse bacterial cells during two 3-minute pulses with ceramic beads using the SpeedMill PLUS (Analytik Jena, Germany). After centrifugation, the supernatant was transferred to new collection tubes just prior to precipitation. We followed the protocol for the remaining steps. We included ten extraction blanks and six standardised communities (ZymoBIOMICS Microbial Community DNA Standard, Zymo Research, Germany).

We amplified the V4 region of the 16S rRNA gene using the 515F-806R primer pair (Fwd: 5'-GTGCCAGCMGCCGCGGTAA-3'; Rvs: 5'- GGACTACHVGGGTWTCTAAT-3') [60] and added Illumina adaptor sequences using the Fluidigm Access Array for Illumina Sequencing (Access Array System for Illumina Sequencing Systems, © Standard Bio Tools, USA). Post purification (NucleoMag NGS clean-up and size select, Macherey-Nagel, Germany) and quantification (QuantiFluor dsDNA System, Promega, USA) the normalized pooled sample library was sequenced as paired-end run on the Illumina MiSeq platform at the Institute for Human Genetics, University Hospital of Bonn. A total of nine PCR controls were included.

The reads were processed with the DADA2 plug-in in QIIME 2 (v2021.8.0, Bolyen et al., 2019), removing primers, denoising reads, detecting and removing chimeras, merging paired-end reads, and differentiating between single amino acid sequence variants (ASVs, Callahan et al., 2016). ASVs were then assigned their taxonomy using SILVA (v138) as reference database [63].

ASVs unassigned at the phylum level or identified to originate from chloroplast or mitochondrial sequences were excluded from subsequent analyses. An unrooted, phylogenetic tree was build using Mafft [64] and FastTree [65]. The tree was rooted in Dendroscope [66] using an archaeon sequence (accession number: KU656649) as the outgroup, which was later removed. Metadata including each sample's sex, age, location, infection status, the CT-value of the respective infection and sampling period, the taxonomy and ASV counts, and the phylogenetic tree were imported into the Rstudio interface of R (v4.3.2, R Core Team, 2022) using the 'phyloseq' package (v1.46.0, McMurdie & Holmes, 2013). All sample processing and statistical analyses were performed in Rstudio.

We first confirmed the community composition of the six standardized microbial community references, which showed no large deviation in amplification across the extraction runs from the expected community composition (Supplementary Figure 1). Next, we pruned unassigned ASVs at the phylum level, ASVs with fewer than 10 reads and phyla with fewer than 0.3% total reads across all samples leaving us with 4,852 ASVs from an original of 10,975. Employing the prevalence-based contamination identification functions from the 'decontam' R package (v1.16) with the default P*-threshold set to 0.1 [69], we identified a possible 163 taxa (3.3%) from the 10 extraction blanks and 165 taxa (3.4%) from the 9 PCR blanks. These taxa were removed. Finally, the decontaminated phyloseq object contained 4,531 taxa compiled from 7,161,284 reads. We plotted alpha-diversity rarefaction curves for each sample with the rarecurve function from the 'vegan' R package (v2.6-4, Oksanen et al., 2022). Based on the curves (Supplementary Figure 2), two fecal samples below a sequencing depth of 5000 reads were eliminated from downstream analyses (including all controls) and one samples missing age information. Hence, a

total of 218 high-quality fecal samples with on average 32,849 reads (±11,198 standard deviation; range: 8,815-62,295 reads) remained.

Statistical analysis

Log-transformed body condition was compared using a linear mixed effect model including sampling location, host sex and infection status while accounting for capture period as random effect on 591 adult *H. caffer D*. *Post-hoc* pairwise comparisons were performed with the 'lmerTest' package (v.3.1.1-3, Kuznetsova et al., 2017). The analysis was repeated for body mass, which yielded similar results [72].

Alpha-diversity metrics (i.e., Observed ASVs, Shannon, and Faith's Phylogenetic diversity) were calculated employing the 'phyloseq' (v1.46.0, McMurdie & Holmes, 2013) and 'picante' package (v1.8.2, Kembel et al., 2010) for samples rarefied to the sequencing depth of the sample with the lowest reads (i.e., 8815 reads, Supplementary Figure 2, Schloss, 2023; Weiss et al., 2017). While observed ASVs measures actual bacterial ASV richness, Shannon diversity index also accounts for evenness, and Faith's Phylogenetic diversity considers abundance and phylogenetic proximity between ASVs. The effect of sampling locations, host sex, host age and CoV infection status on each metric was then estimated using a linear mixed effect model with capture period as random effect. The observed ASV richness was log-transformed, and Shannon diversity index and Faith's Phylogenetic Diversity were square-rooted to meet normality assumption. Subsequently, we assessed whether each alpha-diversity index correlated with infection intensity (measured as CT-value).

To assess inter-sample differences, we first calculated unweighted and weighted Unifrac-distances as microbial beta-diversity indices on the rarefied data agglomerated to genus level.

Both distances take phylogenetic distance between ASVs into account, but whereas weighted Unifrac considers reads as proxy for ASV abundance, and, thus, represents the structure of a microbial community, unweighted Unifrac treats ASVs as either absent or present and, hence, epitomizes the composition of a microbial community. We used each index separately as response variable in a PERMANOVA to determine changes in centroid position associated with sampling location, host sex, host age and CoV infection status and PERMUtest to assess differences in distance to centroid. Following from this, we extracted the unweighted and weighted distances as matrix from all infected samples and calculated the average distance to other samples in the same infection category. The average distance, therefore, denotes how dissimilar a particular sample is from others. Finally, we correlated the average distance between samples with infection intensity (measured as CT-value).

In order to understand which bacterial genera differed between infection status, we used joint-species distribution modelling. Compared with traditional abundance-based analyses (e.g., ANCOM), joint species distribution models incorporate correlations between bacterial taxa when predicting their abundance with respect to the explanatory variable [76]. Since taxonomic databases remain biased towards identifying microbial taxa from common model organisms, the taxonomic resolution for wildlife gut microbiota at the species level is lacking [77, 78]. As to avoid spurious results, we agglomerated reads at the genus level and restricted our analysis to genera with a prevalence >50% (i.e., common core, Risely, 2020). The abundance was centered log-transformed (clr, Quinn et al., 2019). Finally, we constructed a generalized linear latent variable model (GLLVM) using the 'gllvm' package [76]. We evaluated multivariate microbial abundance data using the joint model with the same model structure as for testing alpha- and beta-diversity, meaning that sampling location, host age, sex and infection status, were kept as

main explanatory variables and capture period was used as random effect. Additionally, we accounted for sequencing depth and specified a negative binomial distribution for our response variable.

For those genera that were identified to occur more or less frequent in samples from bats infected with *Hibecovirus* CoV-2B, we wanted to ascertain whether their abundance was linked to infection intensity when compared to uninfected bats. In other words, we aimed to understand whether there is a linear or non-linear relationship with CT-value. We constructed generalised additive models with the clr-transformed abundances (i.e., reads) as response and sampling location, sex and age as categorical explanatory variables. The *Hibecovirus* 2B CT-value was included as smooth term. Sequencing depth was included as smooth term as way to control for differences in sequencing performance between samples. Model fit was assessed using gam.check() function of the 'mgcv' package [81] and we visualized the model results using plot_smooths() from the 'tidymv' package [82].

Results

Body condition

Only individuals infected with the *Hibecovirus* CoV-2B had a significant lower body condition than uninfected bats and those infected with the *Duvinacovirus* CoV-229E-like (Table 1). Bats infected with the other *Hibecovirus* CoV-2Bbasal show a non-significant tendency for a lower body condition than uninfected bats (Table 1c). Sex had no significant influence on body condition, the highest body condition was found in the cave Forikrom.

Gut microbial community composition

The gut microbial community was dominated by *Bacillota* (67.0%; formerly known as *Firmicutes*) represented mainly by members of bacterial class *Bacilli*, and *Pseudomonadota* (27.2%; formerly known as *Proteobacteria*) by enlarge ascribed to *Gammaproteobacteria* (Figure 1A). The 28 common core genera (i.e., found in more than 50% of samples) made up 86.2% of reads per sample (±15.3% standard deviation) with 71.2% reads belonging to *Lactococcus*, *Streptococcus*, *Enterococcus*, *Gemella* and *Paeniclostridium*. Hierarchical clustering showed a weak similarity in the unrarefied gut microbial composition of samples with shared infection status (e.g., CoV-229E infected bats; Figure 1B).

Alpha- and beta-diversity

When comparing (rarefied) gut microbial alpha-diversity, infection status appeared as the single best explanatory variable (Supplementary Table 1). Post-hoc testing confirmed our prediction in that infections with *Hibecovirus* CoV-2B altered the gut microbial diversity (Figure 2A; Supplementary Figure 3A, B): microbial diversity was lower for bats infected with CoV-2B than for uninfected, *Hibecovirus* CoV-2Bbasal or *Duvinacovirus* CoV-229E-like-infected bats irrespective of the alpha-diversity index at hand ($F_{3,214}$=4.40, p=0.005; Supplementary Table 1 for Observed ASVs and Shannon Diversity Index). This prompted us to test whether recorded rt-PCR cycle threshold (CT) values – a proxy for infection intensity – altered alpha-diversity. Indeed, the CT-values of bats infected with *Hibecovirus* CoV-2B were positively correlated with alpha-diversity (Figure 2B). In other words, alpha-diversity declined with infection intensity. However, there was no change observed in alpha-diversity with infection intensity for infections caused by the other two CoVs (Figure 2C, D).

In addition, the centroids of the (rarefied) gut microbial beta-diversity in bats infected with CoVs shifted away from the centroid of uninfected bats analyzed (Figure 2E; unweighted Unifrac measuring composition: R2=0.043, F=3.32, p=0.001; weighted Unifrac measuring structure: R2=0.026, F=2.04, p=0.028; Supplementary Figure 4). The unweighted Unifrac distances calculated from samples of *Duvinacovirus* CoV-229E-like infected bats were on average less dispersed than uninfected and *Hibecovirus* CoV-2B infected bats, and *Hibecovirus* 2Bbasal infected bats were less dispersed than uninfected bats (Supplementary Figure 4). Samples did not differ in dispersion when beta-diversity was calculated as weighted Unifrac distances (Supplementary Figure 4). Host sex and age had no effect on the gut microbial composition and structure, whereas sampling location explained some variation in unweighted Unifrac dissimilarity between samples albeit less than infection status (Supplementary Table 2). Substituting the categorical infection status term once more with the continuous CT-value, we discovered that unweighted Unifrac distances negatively correlated with increased infection intensity only in *Hibecovirus* CoV-2B infected bats (Figure 2F-H), but had no effect on weighted Unifrac distances (Supplementary Table 3).

Joint-species distribution modelling and generalized additive models

For a more detailed understanding about which gut bacterial members varied between infections we then employed a joint species distribution model on the most common bacterial genera. Of the 28 core genera, ten varied significantly between uninfected and CoV-2B infected bats (Figure 3A; Supplementary Table 4). Among others, bacteria of the genus *Mycoplasma* and *Staphylococcus* were more abundant in the gut microbial community of CoV-2B infected bats. *Christensellaceae* R-7 group and *Alistipes* were less frequently detected in infected bats. By

contrast, fewer genera were associated with the other two CoV infections (Supplementary Table 4). Noteworthy is that the abundance of *Gemella* declined in all infected bats. Few genera differed between locations or among the sexes, whereas several genera were found more or less abundant in subadults than in adults (Supplementary Figure 5).

We predicted that several of these genera either decrease or increase with CoV-2B infection intensity, and constructed generalized additive models to test for linear and non-linear relationships with the CT-values. As expected, *Mycoplasma* and *Staphylococcus* were most frequent in samples from bats with the lowest CT-values and declined linearly in abundance in relation to uninfected bats (Figure 3B, C). Vice versa, members of the genera *Christensellaceae* R-7 group, *Alistipes*, and *Candidatus Solerferrea*, by comparison, were less prevalent at low CT-values when compared to uninfected bats (Figure 3F, G, H; Supplementary Table 5). Other genera, including the fourth and fifth most common core genera *Gemella* and *Paeniclostridium*, showed no significant linear change with infection intensity (Figure 3E, I, Supplementary Table 5).

Discussion

Bats host a variety of viruses, but few records of health repercussions exist [18, 83, 84]. We tested whether infections with either of three bat CoVs altered body condition and changed the gut microbial community in wild *H. caffer D*, and predicted to observe the most prominent responses to infection with the *Hibecovirus* CoV-2B, which this bat species seems susceptible to [51, 53]. Our observations yielded three insights: 1) The impact on body condition and the gut microbial community seems to be virus dependent with CoV-2B infections linked to reduced body condition and microbial diversity while the other *Hibecovirus* CoV-2Bbasal and the *Duvinacovirus* CoV-229E-like had no detectable effect; 2) the gut bacterial diversity declined and

the community composition became more dissimilar among the more severely CoV-2B infected bats; and 3) the gut microbial community of CoV-2B infected bats was enriched with potentially pathogenic bacterial genera and depauperated of health-associated taxa. These findings showcase how pathogen reservoirs, and specifically bats respond to virus infections but also underscore that responses are likely specific to the co-evolutionary relationship between host and virus.

H. caffer D infected with the distantly SARS-related *Hibecovirus* CoV-2B presented a lower body condition, a reduced gut microbial diversity and a shift in gut microbial composition. A reduction in body condition was also seen in Hendra virus-positive Black flying foxes (*Pteropus alecto*, [19]) and CoV-positive Lyle's flying foxes (*P. lylei*, [23]). This weight loss may not actually be caused by the infection but rather due to an increased probability of infection during periods of seasonal weight loss in flying foxes [24]. Seasonality in CoV shedding is also known from some studies but absent in others (e.g.,[85, 86]). Seasonal variation in insect prey could similarly explain changes in the gut microbiota [87]. However, we accounted for sample period statistically and would otherwise expect to see similar results for individuals infected with any of the other two CoVs, which tend to have overlapping periods of high prevalence [55]. This is not the case. Infections with the most recent ancestor to the HCoV-229E and the more basal *Hibecovirus* demonstrated no apparent differences in body condition or gut microbial community. Host responses to infection are therefore likely virus dependent. Furthermore, gut dysbiosis may not even translate into changes in body condition. For example, in Astrovirus infected Jamaican fruit bats body condition remained unaffected in spite of a reshuffling of the taxonomic gut microbial profile [41]. This raises the possibility that gut microbial dysbiosis is an invisible and often overlooked health marker in epidemiological studies on bats.

Unlike the previous work on the impact of Astrovirus infections on the gut microbial community [41], we demonstrated that alpha- and beta-diversity correlated with infection intensity. These findings imply a quantifiable dimension to the Anna-Karenina Principle [7] where viral infection intensity governs the level of gut microbial idiosyncrasy. During the latent infection with the simian immunodeficiency virus chimpanzees also show little to no differences in their gut microbial composition, but the gut microbial composition was severely changed in apes dying from an AIDS-like immunopathology [11]. The gut microbial community of patients with hepatitis C also progressively changes with disease severity [88], and hamsters and macaques clinically infected with SARS-CoV-2 showed trends towards higher gut microbial dissimilarity over the course of the disease [45, 46]. Thus, our finding that microbial diversity and dissimilarity scales with infection intensity is likely. Nevertheless, without repeated samples from the same bat we cannot be certain at which time point of the infection (i.e., pre-, post- or during CT-peak) the sample was taken [26], and the observation remains correlational.

The gut microbial community consisted largely of *Bacillota* and *Pseudomonadota*, closely matching the composition of other insectivorous bats [29, 35, 89]. Yet, among the 28 core genera many showed varying abundances dependent on infection status. Several presumably beneficial bacteria belonging to the order of *Bacteroidales* and *Clostridiales* declined in abundance in CoV-2B infected bats. Members of these bacterial orders were depleted in patients with more severe Covid-19 symptoms compared to patients presenting only mild symptoms [90]. The abundance of several members of the *Christensenellaceae* R-7 group were also negatively correlated with SARS-CoV-2 viral load and inflammatory markers in macaques [46]. At the same time, potentially pathogenic bacteria become enriched in CoV-2B infected bats. The genus *Mycoplasma*, which features bacterial species pathogenic to humans (e.g.

384 *Mycoplasma pneumoniae*), livestock (e.g., *Mycoplasma bovis*) and wild animals (e.g.,
385 *Mycoplasma ovipneumoniae*, [91]), was more abundant in CoV-2B positive bats and increased
386 linearly with infection intensity. *Mycoplasma* was also common in Jamaican fruit bats infected
387 with an Astrovirus [41, 92]. An open question remains whether such taxonomic changes render
388 the gut microbial community functionally incapacitated, which is ideally addressed with multi-
389 omics.

390 Our line of argument rests on the assumption that a more dysbiotic state marked by a loss of
391 overall bacterial diversity, increased idiosyncrasy, and an enrichment of potentially pathogenic
392 members at the expense of beneficial bacteria is a consequence of the *Hibecovirus* 2B infection.
393 Equally feasible is that stress altered the gut microbial diversity initially and diminished its ability
394 to withstand subsequent colonialization by *Hibecovirus* 2B and, hence, increase the hosts
395 susceptibility to the virus (e.g., nutritional stress [93, 94], asynchronous co-infections [59] and
396 human disturbance [95]). This explanation is challenged by the finding that infections with the
397 *Duvinacovirus* and *Hibecovirus* 2Bbasal reach similar intensities, regardless of variations in the
398 host's gut microbial diversity. Without repeated sampling from bats as they progress through
399 the infection and a functional profile of gut symbionts, we are unable to test whether the
400 observed changes in the taxonomic memberships are due to the infection, or even whether they
401 have ramifications for microbiome-mediated metabolic and immunological functions [17, 26,
402 96], and ultimately, host fitness [5]. Ideally, future studies could non-invasively probe for
403 physiological markers that play a role in mediating host immunity and communicating with gut
404 bacteria (e.g., short chain fatty acids, IgA/IgG, mucin; [97, 98]), and new multi-omics approaches
405 may provide a higher resolution of the diversity of pathogens infecting bats and other hosts [99,
406 100].

Taken together, our results demonstrate a link between infection with the *Hibecovirus* CoV-2B and changes in the gut microbial community of a putative virus reservoir. We provide evidence that the gut bacterial diversity declined and the community composition became more dissimilar among the more severely infected bats in line with expectations based on the Anna-Karenina principle [7]. Furthermore, potentially pathogenic bacteria took hold, while common symbionts declined in the depauperated gut microbial community of acutely infected bats. If gut dysbiosis was a consequence of more severe infections, as we propose here, this might lead to poorer coverage of bacterial services hosts rely upon [13]. In turn, reservoir species, such as bats, may still suffer from viral infections via an phenotypically invisible health indicator – the microbiota [3, 31].

Data availability

Metagenome data can be accessed from NCBI under BioProject no. PRJNA1096136. Meta data can be accessed from github (https://github.com/DominikWSchmid/GhanaHippos_CoV_microbiome).

Code availability

Workflow and code are freely accessible from github (https://github.com/DominikWSchmid/GhanaHippos_CoV_microbiome).

Acknowledgments

We want to thank S. Heilmann-Heimbach and A. Heimbach for their NGS support, and Kunal Jani for feedback on an early version of the manuscript. We thank two anonymous reviewers for their constructive feedback.

Funding

This work was supported by the DFG Research Infrastructure West German Genome Center, project 407493903, as part of the Next Generation Sequencing Competence Network, project 423957469. Next Generation Sequencing was carried out at the production West German Genome Center Düsseldorf. Simone Sommer received the DFG grant SO 428/17-1 as part of the DFG Sequencing call #2.

Conflict of Interests: The authors declare no competing interests.

References

1. Le Chatelier E, Nielsen T, Qin J, Prifti E, Hildebrand F, Falony G, et al. Richness of human gut microbiome correlates with metabolic markers. *Nature* 2013; **500**: 541–546.
2. Sommer F, Anderson JM, Bharti R, Raes J, Rosenstiel P. The resilience of the intestinal microbiota influences health and disease. *Nat Rev Microbiol* 2017; **15**: 630–638.
3. Trevelline BK, Fontaine SS, Hartup BK, Kohl KD. Conservation biology needs a microbial renaissance: a call for the consideration of host-associated microbiota in wildlife management practices. *Proceedings of the Royal Society B: Biological Sciences* 2019; **286**: 20182448.
4. Härer A, Thompson KA, Schluter D, Rennison DJ. Associations Between Gut Microbiota Diversity and a Host Fitness Proxy in a Naturalistic Experiment Using Threespine Stickleback Fish. *Molecular Ecology* ; **n/a**: e17571.

5. Risely A, Müller-Klein N, Schmid DW, Wilhelm K, Clutton-Brock TH, Manser MB, et al. Climate change drives loss of bacterial gut mutualists at the expense of host survival in wild meerkats. *Global Change Biology* 2023; **29**: 5816–5828.

6. Worsley SF, Davies CS, Mannarelli M-E, Hutchings MI, Komdeur J, Burke T, et al. Gut microbiome composition, not alpha diversity, is associated with survival in a natural vertebrate population. *Animal Microbiome* 2021; **3**: 84.

7. Zaneveld JR, McMinds R, Vega Thurber R. Stress and stability: applying the Anna Karenina principle to animal microbiomes. *Nat Microbiol* 2017; **2**: 17121.

8. Baldini F, Hertel J, Sandt E, Thinnes CC, Neuberger-Castillo L, Pavelka L, et al. Parkinson's disease-associated alterations of the gut microbiome predict disease-relevant changes in metabolic functions. *BMC Biol* 2020; **18**: 62.

9. Brestoff JR, Artis D. Commensal bacteria at the interface of host metabolism and the immune system. *Nat Immunol* 2013; **14**: 676–684.

10. Rooks MG, Veiga P, Wardwell-Scott LH, Tickle T, Segata N, Michaud M, et al. Gut microbiome composition and function in experimental colitis during active disease and treatment-induced remission. *The ISME Journal* 2014; **8**: 1403–1417.

11. Barbian HJ, Li Y, Ramirez M, Klase Z, Lipende I, Mjungu D, et al. Destabilization of the gut microbiome marks the end-stage of simian immunodeficiency virus infection in wild chimpanzees. *American J Primatol* 2018; **80**: e22515.

12. McKenna P, Hoffmann C, Minkah N, Aye PP, Lackner A, Liu Z, et al. The Macaque Gut Microbiome in Health, Lentiviral Infection, and Chronic Enterocolitis. *PLoS Pathog* 2008; **4**: e20.

13. Wilmes P, Martin-Gallausiaux C, Ostaszewski M, Aho VT, Novikova PV, Laczny CC, et al. The gut microbiome molecular complex in human health and disease. *Cell Host & Microbe* 2022; **30**: 1201–1206.

14. Ganz HH, Doroud L, Firl AJ, Hird SM, Eisen JA, Boyce WM. Community-Level Differences in the Microbiome of Healthy Wild Mallards and Those Infected by Influenza A Viruses. *mSystems* 2017; **2**: 10.1128/msystems.00188-16.

15. Moeller AH, Shilts M, Li Y, Rudicell RS, Lonsdorf EV, Pusey AE, et al. SIV-Induced Instability of the Chimpanzee Gut Microbiome. *Cell Host & Microbe* 2013; **14**: 340–345.

16. Wasimuddin, Corman VM, Ganzhorn JU, Rakotondranary J, Ratovonamana YR, Drosten C, et al. Adenovirus infection is associated with altered gut microbial communities in a non-human primate. *Sci Rep* 2019; **9**: 13410.

17. Williams CE, Hammer TJ, Williams CL. Diversity alone does not reliably indicate the healthiness of an animal microbiome. *The ISME Journal* 2024; **18**: wrae133.

18. Brook CE, Dobson AP. Bats as 'special' reservoirs for emerging zoonotic pathogens. *Trends in Microbiology* 2015; **23**: 172–180.

19. Edson D, Peel AJ, Huth L, Mayer DG, Vidgen ME, McMichael L, et al. Time of year, age class and body condition predict Hendra virus infection in Australian black flying foxes (Pteropus alecto). *Epidemiol Infect* 2019; **147**: e240.

20. Letko M, Seifert SN, Olival KJ, Plowright RK, Munster VJ. Bat-borne virus diversity, spillover and emergence. *Nat Rev Microbiol* 2020; **18**: 461–471.

21. Li W, Shi Z, Yu M, Ren W, Smith C, Epstein JH, et al. Bats Are Natural Reservoirs of SARS-Like Coronaviruses. *Science* 2005; **310**: 676–679.

22. Mollentze N, Streicker DG. Viral zoonotic risk is homogenous among taxonomic orders of mammalian and avian reservoir hosts. *Proc Natl Acad Sci USA* 2020; **117**: 9423–9430.

23. Wacharapluesadee S, Duengkae P, Chaiyes A, Kaewpom T, Rodpan A, Yingsakmongkon S, et al. Longitudinal study of age-specific pattern of coronavirus infection in Lyle's flying fox (Pteropus lylei) in Thailand. *Virology Journal* 2018; **15**: 38.

24. McMichael L, Edson D, Mayer D, McLaughlin A, Goldspink L, Vidgen ME, et al. Temporal Variation in Physiological Biomarkers in Black Flying-Foxes (Pteropus alecto), Australia. *Ecohealth* 2016; **13**: 49–59.

25. Moreno KR, Weinberg M, Harten L, Salinas Ramos VB, Herrera M. LG, Czirják GÁ, et al. Sick bats stay home alone: fruit bats practice social distancing when faced with an immunological challenge. *Annals of the New York Academy of Sciences* 2021; **1505**: 178–190.

26. Sánchez CA, Phelps KL, Frank HK, Geldenhuys M, Griffiths ME, Jones DN, et al. Advances in understanding bat infection dynamics across biological scales. *Proceedings of the Royal Society B: Biological Sciences* 2024; **291**: 20232823.

27. Ruhs EC, McFerrin K, Jones DN, Cortes-Delgado N, Ravelomanantsoa NAF, Yeoman CJ, et al. Rapid GIT transit time in volant vertebrates, with implications for convergence in microbiome composition. 2024.

28. Klite PD. Intestinal Bacterial Flora and Transit Time of Three Neotropical Bat Species. *Journal of Bacteriology* 1965; **90**: 375–379.

29. Lutz HL, Jackson EW, Webala PW, Babyesiza WS, Kerbis Peterhans JC, Demos TC, et al. Ecology and Host Identity Outweigh Evolutionary History in Shaping the Bat Microbiome. *mSystems* 2019; **4**: e00511-19.

30. Song SJ, Sanders JG, Delsuc F, Metcalf J, Amato K, Taylor MW, et al. Comparative Analyses of Vertebrate Gut Microbiomes Reveal Convergence between Birds and Bats. *mBio* 2020; **11**: 10.1128/mbio.02901-19.

31. Jones DN, Ravelomanantsoa NAF, Yeoman CJ, Plowright RK, Brook CE. Do gastrointestinal microbiomes play a role in bats' unique viral hosting capacity? *Trends in Microbiology* 2022; **30**: 632–642.

32. Williams CE, Fontaine SS. Commentary: The microbial dependence continuum: Towards a comparative physiology approach to understand host reliance on microbes. *Comparative Biochemistry and Physiology Part A: Molecular & Integrative Physiology* 2024; **296**: 111690.

33. Price ER, Brun A, Caviedes-Vidal E, Karasov WH. Digestive Adaptations of Aerial Lifestyles. *Physiology* 2015; **30**: 69–78.

34. Daniel DS, Ng YK, Chua EL, Arumugam Y, Wong WL, Kumaran JV. Isolation and identification of gastrointestinal microbiota from the short-nosed fruit bat Cynopterus brachyotis brachyotis. *Microbiol Res* 2013; **168**: 485–496.

35. Ingala MR, Simmons NB, Dunbar M, Wultsch C, Krampis K, Perkins SL. You are more than what you eat: potentially adaptive enrichment of microbiome functions across bat dietary niches. *anim microbiome* 2021; **3**: 82.

36. Phillips CD, Hanson J, Wilkinson JE, Koenig L, Rees E, Webala P, et al. Microbiome Structural and Functional Interactions across Host Dietary Niche Space. *Integrative and Comparative Biology* 2017; **57**: 743–755.

37. Prem Anand AA, Sripathi K. Digestion of cellulose and xylan by symbiotic bacteria in the intestine of the Indian flying fox (*Pteropus giganteus*). *Comparative Biochemistry and Physiology Part A: Molecular & Integrative Physiology* 2004; **139**: 65–69.

38. Zepeda Mendoza ML, Xiong Z, Escalera-Zamudio M, Runge AK, Thézé J, Streicker D, et al. Hologenomic adaptations underlying the evolution of sanguivory in the common vampire bat. *Nat Ecol Evol* 2018; **2**: 659–668.

39. Berman TS, Weinberg M, Moreno KR, Czirják GÁ, Yovel Y. In sickness and in health: the dynamics of the fruit bat gut microbiota under a bacterial antigen challenge and its association with the immune response. *Front Immunol* 2023; **14**.

40. Liu B, Chen X, Zhou L, Li J, Wang D, Yang W, et al. The gut microbiota of bats confers tolerance to influenza virus (H1N1) infection in mice. *Transboundary and Emerging Diseases* 2022; **69**: e1469–e1487.

41. Wasimuddin, Brändel SD, Tschapka M, Page R, Rasche A, Corman VM, et al. Astrovirus infections induce age-dependent dysbiosis in gut microbiomes of bats. *ISME J* 2018; **12**: 2883–2893.

42. Anthony SJ, Johnson CK, Greig DJ, Kramer S, Che X, Wells H, et al. Global patterns in coronavirus diversity. *Virus Evolution* 2017; **3**.

43. Corman VM, Baldwin HJ, Tateno AF, Zerbinati RM, Annan A, Owusu M, et al. Evidence for an Ancestral Association of Human Coronavirus 229E with Bats. *J Virol* 2015; **89**: 11858–11870.

44. Aljabr W, Alruwaili M, Penrice-Randal R, Alrezaihi A, Harrison AJ, Ryan Y, et al. Amplicon and Metagenomic Analysis of Middle East Respiratory Syndrome (MERS) Coronavirus and

the Microbiome in Patients with Severe MERS. *mSphere* 2021; **6**: 10.1128/msphere.00219-21.

45. Sencio V, Machelart A, Robil C, Benech N, Hoffmann E, Galbert C, et al. Alteration of the gut microbiota following SARS-CoV-2 infection correlates with disease severity in hamsters. *Gut Microbes* 2022; **14**: 2018900.

46. Sokol H, Contreras V, Maisonnasse P, Desmons A, Delache B, Sencio V, et al. SARS-CoV-2 infection in nonhuman primates alters the composition and functional activity of the gut microbiota. *Gut Microbes* 2021; **13**: 1893113.

47. Zuo T, Liu Q, Zhang F, Lui GC-Y, Tso EY, Yeoh YK, et al. Depicting SARS-CoV-2 faecal viral activity in association with gut microbiota composition in patients with COVID-19. *Gut* 2021; **70**: 276–284.

48. Essex M, Millet Pascual-Leone B, Löber U, Kuhring M, Zhang B, Brüning U, et al. Gut microbiota dysbiosis is associated with altered tryptophan metabolism and dysregulated inflammatory response in COVID-19. *npj Biofilms Microbiomes* 2024; **10**: 1–15.

49. Drexler JF, Corman VM, Drosten C. Ecology, evolution and classification of bat coronaviruses in the aftermath of SARS. *Antiviral Research* 2014; **101**: 45–56.

50. Vallo P, Guillén-Servent A, Benda P, Pires DB, Koubek P. Variation of mitochondrial DNA in the Hipposideros caffer complex (Chiroptera: Hipposideridae) and its taxonomic implications. *acta* 2008; **10**: 193–206.

51. Meyer M. Bat species assemblage predicts coronavirus prevalence. *Nature Communications* 2024.

52. Pfefferle S, Oppong S, Drexler JF, Gloza-Rausch F, Ipsen A, Seebens A, et al. Distant Relatives of Severe Acute Respiratory Syndrome Coronavirus and Close Relatives of Human Coronavirus 229E in Bats, Ghana. *Emerg Infect Dis* 2009; **15**: 1377–1384.

53. Schmid DW, Meyer M, Wilhelm K, Tilley T, Link-Hessing T, Fleischer R, et al. MHC class II genes mediate susceptibility and resistance to coronavirus infections in bats. *Molecular Ecology* 2023; **32**: 3989–4002.

54. Sánchez CA, Becker DJ, Teitelbaum CS, Barriga P, Brown LM, Majewska AA, et al. On the relationship between body condition and parasite infection in wildlife: a review and meta-analysis. *Ecology Letters* 2018; **21**: 1869–1884.

55. Meyer M, Melville DW, Baldwin HJ, Wilhelm K, Nkrumah EE, Badu EK, et al. Bat species assemblage predicts coronavirus prevalence. *Nat Commun* 2024; **15**: 2887.

56. Drexler JF, Corman VM, Müller MA, Maganga GD, Vallo P, Binger T, et al. Bats host major mammalian paramyxoviruses. *Nat Commun* 2012; **3**: 796.

57. Annan A, Baldwin HJ, Corman VM, Klose SM, Owusu M, Nkrumah EE, et al. Human Betacoronavirus 2c EMC/2012–related Viruses in Bats, Ghana and Europe. *Emerg Infect Dis* 2013; **19**: 456–459.

58. Drexler JF, Kupfer B, Petersen N, Grotto RMT, Rodrigues SMC, Grywna K, et al. A Novel Diagnostic Target in the Hepatitis C Virus Genome. *PLOS Medicine* 2009; **6**: e1000031.

59. Schmid DW, Fackelmann G, Wasimuddin, Rakotondranary J, Ratovonamana YR, Montero BK, et al. A framework for testing the impact of co-infections on host gut microbiomes. *anim microbiome* 2022; **4**: 48.

60. Caporaso JG, Lauber CL, Walters WA, Berg-Lyons D, Lozupone CA, Turnbaugh PJ, et al. Global patterns of 16S rRNA diversity at a depth of millions of sequences per sample. *Proceedings of the National Academy of Sciences* 2011; **108**: 4516–4522.

61. Bolyen E, Rideout JR, Dillon MR, Bokulich NA, Abnet CC, Al-Ghalith GA, et al. Reproducible, interactive, scalable and extensible microbiome data science using QIIME 2. *Nat Biotechnol* 2019; **37**: 852–857.

62. Callahan BJ, McMurdie PJ, Rosen MJ, Han AW, Johnson AJA, Holmes SP. DADA2: High-resolution sample inference from Illumina amplicon data. *Nat Methods* 2016; **13**: 581–583.

63. Quast C, Pruesse E, Yilmaz P, Gerken J, Schweer T, Yarza P, et al. The SILVA ribosomal RNA gene database project: improved data processing and web-based tools. *Nucleic Acids Research* 2012; **41**: D590–D596.

64. Katoh K, Standley DM. MAFFT Multiple Sequence Alignment Software Version 7: Improvements in Performance and Usability. *Molecular Biology and Evolution* 2013; **30**: 772–780.

65. Price MN, Dehal PS, Arkin AP. FastTree 2 – Approximately Maximum-Likelihood Trees for Large Alignments. *PLoS ONE* 2010; **5**: e9490.

66. Huson DH, Scornavacca C. Dendroscope 3: an interactive tool for rooted phylogenetic trees and networks. *Syst Biol* 2012; **61**: 1061–1067.

67. R Core Team. R: A language and environment for statistical computing. 2022. R Foundation for Statistical Computing.

68. McMurdie PJ, Holmes S. phyloseq: An R Package for Reproducible Interactive Analysis and Graphics of Microbiome Census Data. *PLoS ONE* 2013; **8**: e61217.

69. Davis NM, Proctor DM, Holmes SP, Relman DA, Callahan BJ. Simple statistical identification and removal of contaminant sequences in marker-gene and metagenomics data. *Microbiome* 2018; **6**: 226.

70. Oksanen J, Simpson GL, Blanchet FG, Kindt R, Legendre P, Minchin PR, et al. vegan: Community Ecology Package. 2022.

71. Kuznetsova A, Brockhoff PB, Christensen RHB. lmerTest Package: Tests in Linear Mixed Effects Models. *Journal of Statistical Software* 2017; **82**: 1–26.

72. McGuire LP, Kelly LA, Baloun DE, Boyle WA, Cheng TL, Clerc J, et al. Common condition indices are no more effective than body mass for estimating fat stores in insectivorous bats. *Journal of Mammalogy* 2018; **99**: 1065–1071.

73. Kembel SW, Cowan PD, Helmus MR, Cornwell WK, Morlon H, Ackerly DD, et al. Picante: R tools for integrating phylogenies and ecology. *Bioinformatics* 2010; **26**: 1463–1464.

74. Schloss PD. Waste not, want not: revisiting the analysis that called into question the practice of rarefaction. *mSphere* 2023; **9**: e00355-23.

75. Weiss S, Xu ZZ, Peddada S, Amir A, Bittinger K, Gonzalez A, et al. Normalization and microbial differential abundance strategies depend upon data characteristics. *Microbiome* 2017; **5**: 27.

76. Niku J, Hui FKC, Taskinen S, Warton DI. gllvm: Fast analysis of multivariate abundance data with generalized linear latent variable models in r. *Methods in Ecology and Evolution* 2019; **10**: 2173–2182.

77. Johnson JS, Spakowicz DJ, Hong B-Y, Petersen LM, Demkowicz P, Chen L, et al. Evaluation of 16S rRNA gene sequencing for species and strain-level microbiome analysis. *Nat Commun* 2019; **10**: 5029.

78. Schloss PD, Jenior ML, Koumpouras CC, Westcott SL, Highlander SK. Sequencing 16S rRNA gene fragments using the PacBio SMRT DNA sequencing system. *PeerJ* 2016; **4**: e1869.
79. Risely A. Applying the core microbiome to understand host–microbe systems. *Journal of Animal Ecology* 2020; **89**: 1549–1558.
80. Quinn TP, Erb I, Gloor G, Notredame C, Richardson MF, Crowley TM. A field guide for the compositional analysis of any-omics data. *GigaScience* 2019; **8**: giz107.
81. Wood S. Generalized Additive Models: An Introduction with R, Second Edition (2nd ed.). 2017. Chapman and Hall/CRC.
82. Coretta S, van Rij J, Wieling M. Tidy Model Visualisation for Generalized Additive Models. 2021.
83. Irving AT, Ahn M, Goh G, Anderson DE, Wang L-F. Lessons from the host defences of bats, a unique viral reservoir. *Nature* 2021; **589**: 363–370.
84. Ruiz-Aravena M, McKee C, Gamble A, Lunn T, Morris A, Snedden CE, et al. Ecology, evolution and spillover of coronaviruses from bats. *Nat Rev Microbiol* 2022; **20**: 299–314.
85. Joffrin L, Hoarau AOG, Lagadec E, Torrontegi O, Köster M, Le Minter G, et al. Seasonality of coronavirus shedding in tropical bats. *Royal Society Open Science* 2022; **9**: 211600.
86. Seltmann A, Corman VM, Rasche A, Drosten C, Czirják GÁ, Bernard H, et al. Seasonal Fluctuations of Astrovirus, But Not Coronavirus Shedding in Bats Inhabiting Human-Modified Tropical Forests. *EcoHealth* 2017; **14**: 272–284.
87. Taylor PJ, Monadjem A, Nicolaas Steyn J. Seasonal patterns of habitat use by insectivorous bats in a subtropical African agro-ecosystem dominated by macadamia orchards. *African Journal of Ecology* 2013; **51**: 552–561.

88. Inoue T, Nakayama J, Moriya K, Kawaratani H, Momoda R, Ito K, et al. Gut Dysbiosis Associated With Hepatitis C Virus Infection. *Clinical Infectious Diseases* 2018; **67**: 869–877.

89. Dai W, Leng H, Li J, Li A, Li Z, Zhu Y, et al. The role of host traits and geography in shaping the gut microbiome of insectivorous bats. *mSphere* 2024; **9**: e00087-24.

90. Zuo T, Zhang F, Lui GCY, Yeoh YK, Li AYL, Zhan H, et al. Alterations in Gut Microbiota of Patients With COVID-19 During Time of Hospitalization. *Gastroenterology* 2020; **159**: 944-955.e8.

91. Sumithra TG, Chaturvedi VK, Susan C, Siju SJ, Rai AK, Harish C, et al. Mycoplasmosis in wildlife: a review. *Eur J Wildl Res* 2013; **59**: 769–781.

92. Fleischer R, Schmid DW, Wasimuddin, Brändel SD, Rasche A, Corman VM, et al. Interaction between MHC diversity and constitution, gut microbiota and Astrovirus infections in a neotropical bat. *Molecular Ecology* 2022; **31**: 3342–3359.

93. Eby P, Peel AJ, Hoegh A, Madden W, Giles JR, Hudson PJ, et al. Pathogen spillover driven by rapid changes in bat ecology. *Nature* 2023; **613**: 340–344.

94. Crowley DE, Falvo CA, Benson E, Hedges J, Jutila M, Ezzatpour S, et al. Bats generate lower affinity but higher diversity antibody responses than those of mice, but pathogen-binding capacity increases if protein is restricted in their diet. *PLOS Biology* 2024; **22**: e3002800.

95. Seltmann A, Czirják GÁ, Courtiol A, Bernard H, Struebig MJ, Voigt CC. Habitat disturbance results in chronic stress and impaired health status in forest-dwelling paleotropical bats. *Conserv Physiol* 2017; **5**: cox020.

96. Worsley SF, Videvall E, Harrison XA, Björk JR, Mazel F, Wanelik KM. Probing the functional significance of wild animal microbiomes using omics data. *Functional Ecology* ; **n/a**.

97. Ferreira SCM, Veiga MM, Hofer H, East ML, Czirják GÁ. Noninvasively measured immune responses reflect current parasite infections in a wild carnivore and are linked to longevity. *Ecology and Evolution* 2021; **11**: 7685–7699.

98. Roffler AA, Maurer DP, Lunn TJ, Sironen T, Forbes KM, Schmidt AG. Bat humoral immunity and its role in viral pathogenesis, transmission, and zoonosis. *Front Immunol* 2024; **15**.

99. Donaldson EF, Haskew AN, Gates JE, Huynh J, Moore CJ, Frieman MB. Metagenomic Analysis of the Viromes of Three North American Bat Species: Viral Diversity among Different Bat Species That Share a Common Habitat. *Journal of Virology* 2010; **84**: 13004–13018.

100. Wang J, Pan Y, Yang L, Yang W, Lv K, Luo C, et al. Individual bat virome analysis reveals co-infection and spillover among bats and virus zoonotic potential. *Nat Commun* 2023; **14**: 4079.

Table 1. Summary data, model results and pairwise comparisons of body condition (i.e., mass/forearm length; log-transformed) between cave location, sex and infection status in adult *Hipposideros caffer D.* Significant results are indicated in bold.

a) Body condition	**n**	**BCI**	**standard error**
uninfected	104	0.218	0.002
CoV-2B infected	257	0.213	0.002
CoV-2Bbasal infected	130	0.215	0.001
CoV-229E-like infected	100	0.215	0.002
b) Final model	**dfs**	**F-value**	**p-value**
~ infection status	3, 588	3.26	**0.021**
~ location	4, 588	8.92	**<0.001**
~ sex	1, 582	2.14	0.144

c) Pairwise comparison	Estimate	lower	upper	p-value
uninfected vs 2B	0.030	0.008	0.052	**0.008**
uninfected vs 2Bbasal	0.024	-0.002	0.049	0.066
uninfected vs 229E	0.006	-0.020	0.032	0.648
2B vs. 2Bbasal	-0.006	-0.026	0.014	0.534
2B vs. 229E	-0.024	-0.045	-0.002	**0.030**
2Bbasal vs. 229E	-0.017	-0.041	0.006	1.450

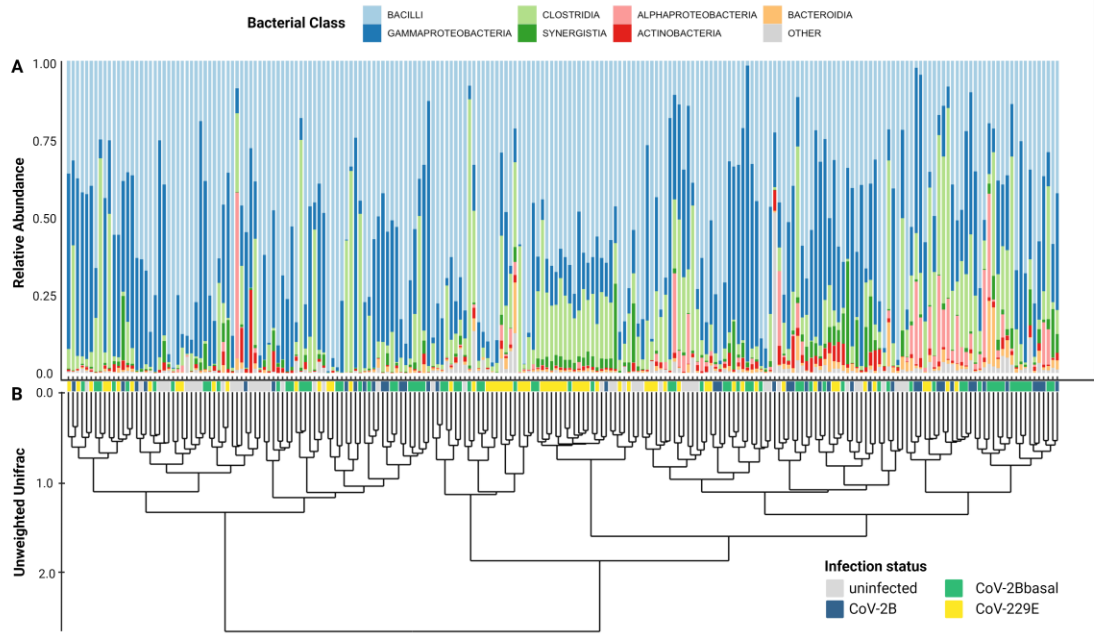

Figure 1. Microbiome composition and hierarchical clustering. A) The gut microbial composition of the 218 fecal samples from *Hipposideros caffer D* with known infection status B) loosely clustered by their (unrarefied) unweighted Unifrac distance-based dissimilarity. Infection status given as colored tiles (grey=uninfected; green=CoV-2Bbasal infected; blue=CoV-2B infected; yellow=CoV-229E infected).

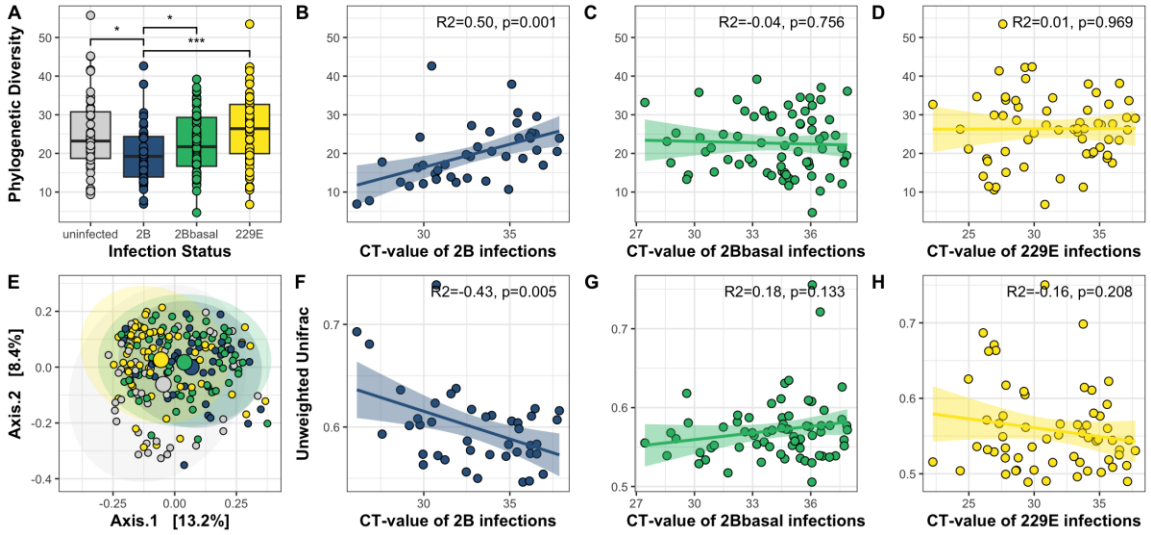

715

716 **Figure 2. Gut microbial alpha- and beta-diversity in relation to infection status and intensity.**

717 A) Differences in gut microbial alpha-diversity (i.e., Faith's Phylogenetic diversity) based on

718 infection status, and B-D) correlational link between alpha diversity and infection intensity of

719 either CoV infection. E) Grouping of gut microbial composition based on beta-diversity (i.e.,

720 rarefied unweighted Unifrac distances calculated from reads agglomerated to bacterial genus),

721 and F-H) correlational link between beta-diversity and infection intensity of either CoV infection.

722 Asterix indicate level of significance: * < 0.05, ** < 0.01, *** <0.001. Colors reflect infection

723 status (grey=uninfected; green=CoV-2Bbasal infected; blue=CoV-2B infected; yellow=CoV-229E

724 infected) and larger points depict respective group centroids.

725

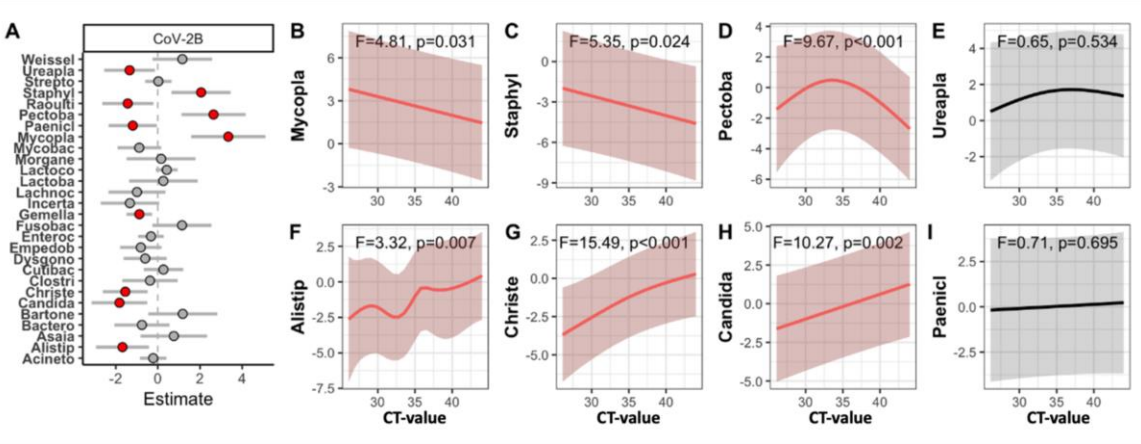

726

727 **Figure 3. Variation in specific taxa abundance in relation to CoV infections.** A) Generalized

728 linear latent variable model indicating which common gut bacterial genera (prevalence > 0.5)

729 are found significantly (* $p < 0.05$, dots colored red) more or less common in CoV-2B infected *H.*

730 *caffer D* than in uninfected bats, and B-I) model estimates from generalized additive models

731 demonstrating significant (in red) relationships between the abundance of bacterial genera and

732 infection intensity. Abbreviations: Weissel=*Weissella*; Ureapla=*Ureaplasma*;

733 Strepto=*Streptococcus*; Staphyl=*Staphylococcus*; Raoulti=*Raoultibacter*; Pectoba=

734 *Pectobacterium*; Paenicl=*Peniclostridium*; Mycopla=*Mycoplasma*; Mycobac=*Mycobacterium*;

735 Morgane=*Morganella*; Lactoco=*Lactococcus*; Lactoba=*Lactobacillus*;

736 Lachnoc=*Lachnoclostridium*; Incerta=*Incertae Sedis*; Fusobac=*Fusobacterium*;

737 Enteroc=*Enterococcus*; Dysgono=*Dysgonomonas*;; Clostri=*Clostridium sensu stricto 1*;

738 Christe=*Christensenellaceae R-7 group*; Candida = *Candidatus Soleaferrea*; Bartone=*Bartonella*;

739 Bactero=*Bacteroides*; Alistip=*Alistipes*; Acineto=*Acinetobacter*.